



Investigation of the Response Characteristics of Masonry Wall Structures under Multi-Cloud Explosion Conditions

Zikai Zhou * and Zhongqi Wang

Beijing Institute of Technology, Beijing, 100081, China

*3120220307@bit.edu.cn

Abstract. This study examines the response characteristics and damage mechanisms of masonry wall structures subjected to multi-cloud explosion conditions, emphasizing structural vulnerability and risk under explosive loads. Through numerical modeling and experimental analysis, pressure, displacement, stress, and damage distribution are investigated across various explosion regions. The results indicate that the complex partitioning of over-pressure fields in multi-point cloud explosions leads to distinct response patterns in single-peak wave zones, multi-peak wave zones, and Mach zones. In the single-peak wave zone, the over-pressure peak reaches 0.4 MPa with minor oscillations, while the multi-peak wave zone exhibits a complex pressure pattern with intensified impact. The Mach zone is characterized by pronounced Mach reflection effects. Additionally, the study identifies damage patterns in masonry walls positioned at the periphery of the cloud zone and under single-point cloud explosion conditions, providing valuable insights into blast-resistant design and structural safety assessment.

Keywords: Multi-cloud explosion; Masonry wall structure; Response characteristics; Structural vulnerability; Blast resistance

1 Introduction

Explosion incidents in industrial and military environments pose significant risks to both personnel and infrastructure. Multi-cloud explosions, characterized by the near-simultaneous detonation of multiple explosive sources, generate intricate overpressure fields that can lead to severe structural damage. As masonry walls are commonly used in construction, understanding their behavior under these conditions is essential for improving blast resistance and enhancing safety.

Extensive research has been conducted on explosion dynamics, forming a foundation for this study. Henrych J. [1] provided a comprehensive analysis of explosion dynamics, while Brode H.L. [2] developed numerical models for spherical blast waves, significantly advancing shock wave propagation studies. Zhao Xingyu et al. [3] refined JWL equation-of-state parameters for fuel-air explosives, enhancing the accuracy of cloud detonation simulations. Additionally, Zhang Kefan [4] investigated multi-point initiation structures, offering insights into cloud explosion complexity.

Research on structural responses to explosions has advanced significantly. Grisaro et al. [5] established a correlation between structural kinetic energy and explosive energy, deriving a refined TNT equivalence coefficient. Zhou Hu et al. [6] investigated thermal enhancement effects on blast loads through TNT explosion experiments in enclosed chambers, proposing a chamber-specific TNT equivalence method. Case studies by Jiang Wenbin et al. [7] and Cheng Shuo et al. [8] provide empirical insights, while Lang Lin et al. [9] examined structural responses under impact and blast loads, further refining explosion impact assessments.

2 Analysis of the Explosion Response of Masonry Walls at the Edge of the Multi-Cloud Zone

2.1 Experimental Setup

To evaluate masonry wall responses in cloud explosion environments, experiments were conducted with walls partially located within the cloud zone. The cloud spacing was set at 2.5 times the over-pressure coverage radius, corresponding to a cloud diameter of 5600 mm and a 14-meter distance between two explosive sources. A localized grid refinement was applied near the cloud zone, while coarser grids were used for the outer regions.

Under explosion conditions, pressures ranged from 1 to 2 MPa within the cloud zone, rapidly decreasing beyond it. The explosion-facing side of the masonry wall was positioned at the cloud zone boundary, while the remaining section was outside. This configuration facilitated failure point analysis and provided data for blast-resistant design. As shown in Figure 1, the load effects on masonry walls vary significantly with position.

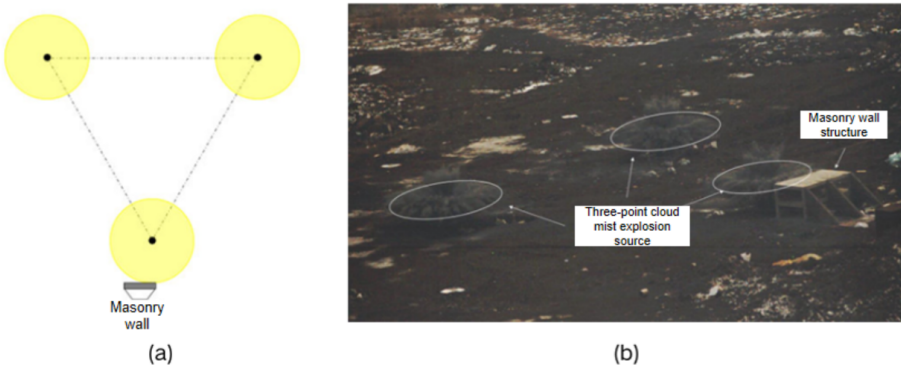


Fig. 1. Comparison of Load Effects on Masonry Walls at Different Positions under Single-Point Cloud Explosion

2.2 Material Parameters and Model Configuration

A finite element model was developed using the BRICK module in AUTODYN. The concrete frame was assigned CONC140MPa, masonry bricks were modeled as CONC35MPa, and mortar was represented by SAND material. Material properties included compressive strength, tensile strength, shear strength, density, and compaction parameters. Specifically, the masonry wall was constructed with standard solid clay bricks (approximately 240 mm × 115 mm × 53 mm each) laid in a running bond pattern using a 1:3 cement–sand mortar. The bricks have an average compressive strength of ~30 MPa, and the mortar has a compressive strength of ~10 MPa with ~10 mm thick joints. The total wall thickness is 240 mm, representing a typical unreinforced singlewythe masonry wall. These material and construction characteristics significantly influence blast resistance: stronger bricks and mortar and good brick–mortar bonding improve the wall's ability to withstand shock waves, whereas weak mortar or poor workmanship (e.g. uneven joints) can create weak planes that reduce blast performance.

Boundary conditions included common-node coupling constraints between air and explosive materials and among structural components. The ground was assigned a fully reflective boundary, while non-reflective outflow conditions simulated a semi-infinite air domain. In Figure 2 illustrates the numerical calculation model and the numbering of wall segments.

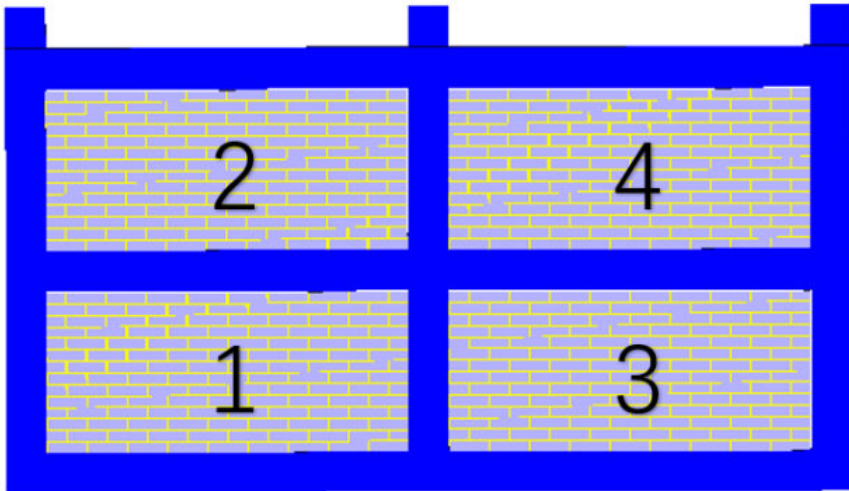


Fig. 2. Numerical Calculation Model and Wall Numbering

2.3 Damage Situation and Analysis

A comparison between numerical and experimental results demonstrated strong consistency. Cracks first appeared at 0.5 ms, indicating initial shock-wave-induced damage. By 1.5 ms, cratering emerged, suggesting progressive energy impact. At 3–4 ms,

crater expansion further reflected cumulative damage effects. The final crack patterns observed in the physical tests closely matched the simulated damage contours. Additionally, the measured peak over-pressure on the wall in the experiment differed by less than 5% from the simulation, confirming the numerical model’s validity in predicting blast-induced damage. The damage characteristics can be seen in Figure 3, which displays simulation results.

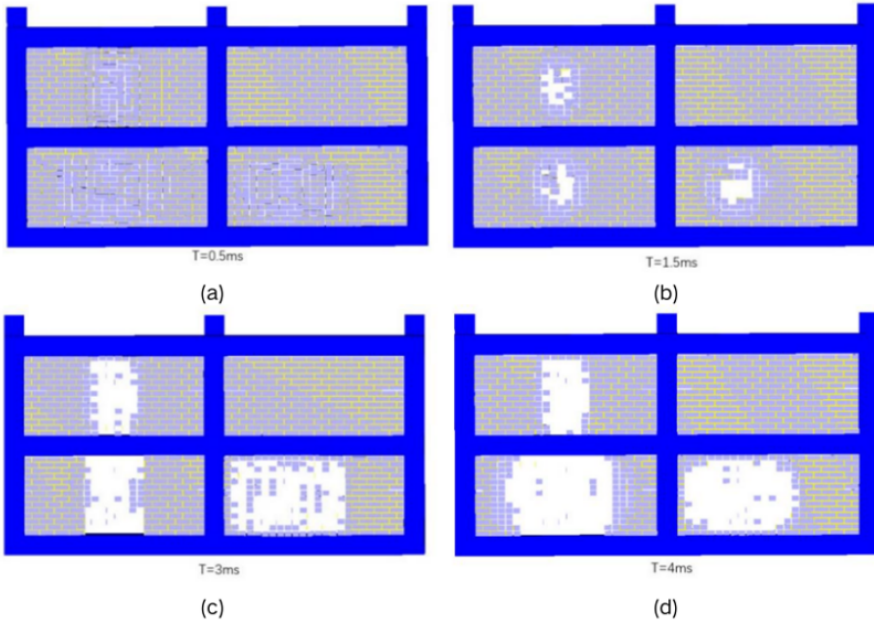


Fig. 3. Numerical Calculation Results

Damage distribution varied significantly:

- Wall 1, near the cloud zone and ground, absorbed nearly all shock energy, resulting in severe destruction.
- Wall 2, adjacent to the cloud zone but elevated, experienced moderate damage (~25% of the surface) due to dissipated energy.
- Wall 3, near the ground but outside the cloud zone, exhibited damage on the cloud-facing side, affecting 50%–75% of the surface.
- Wall 4, elevated and distant from the cloud zone, remained largely undamaged.

Figure 4 compares the numerical and experimental results, showing high consistency.

These findings highlight the correlation between structural positioning and explosion energy distribution. Walls near the cloud zone and in contact with the ground are more vulnerable to high-intensity shock waves, whereas elevated or distant walls experience lower impact.



Fig. 4. Numerical Calculation Results and Experimental Results

3 Conclusion and Outlook

1. Key Findings on Structural Response: Significant variations in damage levels were observed. Walls closer to the cloud zone and in contact with the ground suffered severe damage, while those farther away or elevated remained relatively intact. This underscores the strong relationship between explosion energy distribution and structural positioning, guiding optimized protective measures.

2. Influence of Single-Point Cloud Explosion: The distance between a masonry wall and the cloud zone critically affects reflected shock wave intensity, influencing structural vulnerability. As distance increases, shock wave intensity diminishes, transitioning from a multi-peak to a single-peak wave load. These insights enhance risk assessment frameworks and predictive safety models.

3. Recommendations for Urban Planning and Building Design: Based on these findings, urban planning and building codes should integrate blast-resilience considerations for areas at risk of fuel–air explosions. For instance, safe separation distances should be mandated between potential explosion sources (e.g. industrial fuel storage or chemical facilities) and nearby buildings. Additionally, building design codes may require that masonry walls in such high-risk facilities be reinforced or constructed with blast-resistant details and materials to prevent catastrophic failure. Implementing these measures will reduce the vulnerability of masonry structures and enhance public safety in explosion-prone environments.

This study provides a foundation for designing blast-resistant structures and assessing building safety under multi-cloud explosion hazards. However, the numerical simulation has certain limitations due to idealized modeling assumptions. For instance, material properties were assumed homogeneous (without explicitly accounting for strain-rate effects) and the brick–mortar interface was modeled as perfectly bonded, which may not capture actual joint failures. Additionally, boundary conditions such as the fully reflective ground surface simplify real soil behavior. These assumptions can introduce uncertainty in the predicted response. Therefore, future work should address these issues by incorporating more realistic material models (e.g. including strain-rate dependent strength and allowing brick–mortar delamination) and validating simulations against additional experimental or field data. Future research should also explore

diverse masonry materials, more complex explosion scenarios, and long-term performance considerations to improve risk management and advance blast protection technologies. Furthermore, future research should investigate the potential of integrating data-driven methods such as machine learning to predict damage patterns in masonry walls under varying explosion conditions. Such approaches could enhance predictive capabilities and inform more resilient structural design strategies tailored for diverse urban scenarios.

References

1. Henrych J. The Dynamics of explosion and its Use [M]. Amsterdam: Elsevier, 1979.
2. Brode H L .Numerical Solutions of Spherical Blast Waves[J].Journal of Applied Physics, 1955, 26(6):766-775.
3. Zhao Xingyu, Bai Chunhua, Yao Jian, et al. Calculation of JWL Equation of State Parameters for Detonation Products of Fuel-Air Explosives[J]. Acta Armamentarii, 2020(010):041.
4. Zhang Kefan. Research on the Fracture Mechanism and Laws of Flat Plate/Spherical Segment Structures under Multi-Point Initiation[D]. National University of Defense Technology, 2018.
5. Grisaro H Y , Edri I E , Rigby S .TNT equivalency analysis of specific impulse distribution from close-in detonations[J].International Journal of Protective Structures, 2020.
6. Zhou Hu, Kong Xiangshao, Luo Feng, Cao Yuhang, Zheng Cheng, Wu Weiguo. TNT Equivalent Method for Internal Explosion in Cabin Based on Structural Response[J]. Chinese Journal of Ship Research, 2024, 19(3): 86-95.
7. Jiang Wenbin, Chen Yong, Peng Fei. Estimation of the Explosion Yield of the Xiangshui Chemical Plant in Jiangsu in March 2019[J]. Chinese Journal of Geophysics, 2020, 63(2):10.
8. Cheng Shuo, Yang Fuqiang. Statistics and Grey Relational Analysis of Hazardous Chemical Accidents in China from 2011 to 2020[J]. Applied Chemical Industry, 2023, 52(1):193-198.
9. Lin Lang; Zhenwu Luo, Quan Yuan, Zheming ZhuCA2, Lei Zhou; Qian Xu, Xuebing Tang, Hongxia Gao, Jixing Cao, Zihong Gan. Crack arrest characteristics and dynamic fracture parameters of moving cracks encountering double holes under impact loads[J].International Journal of Impact Engineering,2025,Vol.195: 105158

Open Access This chapter is licensed under the terms of the Creative Commons Attribution-NonCommercial 4.0 International License (<http://creativecommons.org/licenses/by-nc/4.0/>), which permits any noncommercial use, sharing, adaptation, distribution and reproduction in any medium or format, as long as you give appropriate credit to the original author(s) and the source, provide a link to the Creative Commons license and indicate if changes were made.

The images or other third party material in this chapter are included in the chapter's Creative Commons license, unless indicated otherwise in a credit line to the material. If material is not included in the chapter's Creative Commons license and your intended use is not permitted by statutory regulation or exceeds the permitted use, you will need to obtain permission directly from the copyright holder.

